DGA 1005 Literature Review

André CORRÊA

ABSTRACT

Joining has proved to be a critical step in the manufacturing of large and complex composite structures. Traditional joining methods are feasible but not ideal, as they can induce imperfections and consequently degrade the mechanical performance of the composite structure.

Thus, welding is found to be a suitable assembling process applied to thermoplastic composites, overcoming some limitations from traditional assembling methods. Consolidation is one of the key phases of thermoplastic welding in which external pressure and temperature are applied in order to develop, simultaneously, two main phenomena: (I) intimate contact between the adherents and (II) polymer healing across the weld interface.

Even though thermoplastic welding is already successfully employed in the aerospace segment, the industry still urges for predictable, reliable and robust welding models. Thus the current work aims to bring a literature review about the consolidation step of thermoplastic welding process.

Keywords: Consolidation, Thermoplastic, Thermoplastic Welding, Joint/Joining

TABLE OF CONTENTS

Page

LIST OF TABLES

Page

LIST OF FIGURES

Page

LIST OF ABREVIATIONS

FRP	Fibre Reinforced Polymer
ED	Energy Director
HE	Heating Element
RW	Resistance Welding
IW	Induction Welding
UW	Ultrasonic Welding

LIST OF SYMBOLS AND UNITS OF MEASUREMENTS

D_{ic}	Degree of intimate contact
D_h	Degree of healing
ρ	Density
T_g	Glass Temperature
C_p	Heat Capacity
σ	Interlaminar Bond Strenght
h_j	Internal Viscoelastic Stress Variable
T_m	Melting Temperature
χ	Net Interpenetration Depth
τ_j	Relaxation Time
$\Gamma(t)$	Relaxation Function
t_r	Reptation Time
k	Thermal Conductivity
ν	Kinematic Viscosity
μ	Shear Viscosity
t_w	Welding Time

Definitions

Rubbery state - A state in which the polymer is soft, flexible and able to flow.

Intimate Contact - A complete and tight mechanical contact developed between two or more adherents.

Healing - Macromolecular interdiffusion and entanglement in bulk or across interfaces.

Consolidation - A step of the welding process in which pressure and temperature are simultaneously applied in order to develop an intimate contact between adherents and macromolecular interdiffusion across the interface (healing).

Glass Transition Temperature - A defined temperature at which a glassy-rubber transition is observed in an amorphous phase of a thermoplastic polymer.

Melting Temperature - A defined temperature at which the crystalline phase of a semi-crystalline thermoplastic is in its molten state.

Welding - A process through which independent parts are heated, consolidated and cooled down, resulting in a bulk material.

CHAPTER 1

INTRODUCTION

1.1 Motivation and Background

Aviation has long been the focus of public attention for its environmental impact, such as noise, pollutant emissions and, more recently, carbon dioxide (CO2) emissions. In 2009, the entire aviation industry (comprising airlines, aerospace manufacturers, airports, air navigation service providers and business aviation) committed to high-level climate action goals such as (I) improving fuel efficiency by 1.5% per year between 2009 and 2020 and (II) reducing global net aviation carbon emissions by 50% by the year 2050 [International Air Transport Association - IATA (2019)].

This challenging reduction in fuel consumption and greenhouse gas emissions is mainly driven by three factors: a new generation of engines, aerodynamics improvements and extensive usage of composite materials. According to the International Air Transport Association - IATA (2019), the usage of composite materials in primary and secondary structures will reflect up to 4% in fuel reduction from 2019 until 2030 and up to 19% until 2050 (including the usage of materials in engines).

Fibre reinforced polymers (FRPs) are already widely found in the aeronautical industry and represent a technological improvement in the designs of high performance lightweight structures. By combining stiff fibres and a more compliant polymer matrix, they offer improved properties, thanks to their excellent specific strength, stiffness and toughness as shown in Figure 1.1.

The thermal stability of FRPs is mainly driven by the polymeric matrix. Polymeric materials are classified into thermosets and thermoplastics. In the next section, the polymeric nature and behaviour of these two classes will be presented.

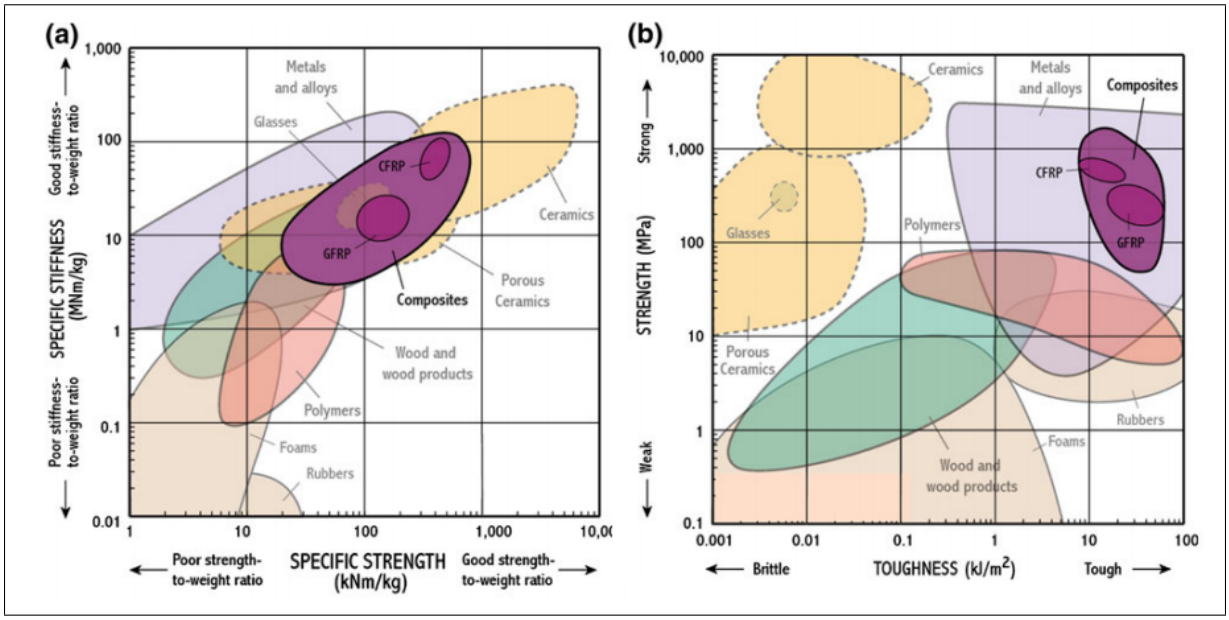

a) Specific Stiffness versus Specific Strength b) Strength versus Fracture Toughness. FRPs have unique strength, stiffness and toughness properties.
Adapted from Llorca *et al.* (2012)

Figure 1.1 Ashby chart comparing the mechanical properties of FRPs with other materials.

1.2 Thermoset and Thermoplastic behaviour

Polymer resins are normally classified according to their temperature response, whether they decompose (thermosets) or soften (thermoplastic) under heating. Thermosets present covalent bonds constraining the chain mobility and therefore do not permitting thermosets to be molten. During the so-called curing process, small molecules are chemically linked, creating complex interconnected networks (Figure 1.2 b) in a hard and permanent rigid state [Bîrca, Gherasim, Grumezescu & Grumezescu (2019)]. Due to the curing process, thermosets are thermally stable below their decomposition temperature, with severe property loss beyond that limit.

Thermoplastics can be considered as ensembles of randomly packed and entangled chains (Figure 1.2 a). Their chain mobility - and therefore their temperature response - is given by the monomer type (repeating unit) and features of the molecular weight [Cervenka (1999)].

Under heating, these entangled chains gain more mobility, enabling the material to soften and flow. Unlike thermosets, this process is reversible and so, thermoplastics can be re-processed, meaning that they can be repaired, remoulded and recycled.

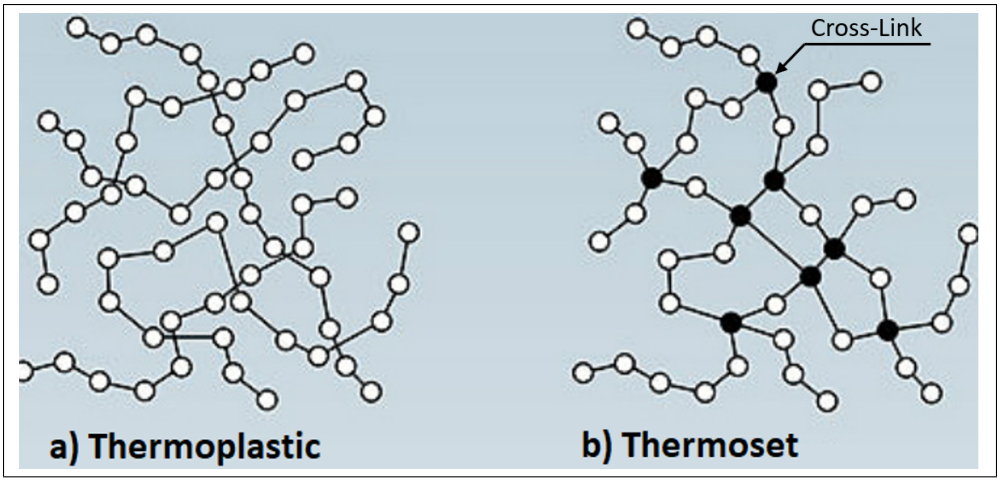

a) Thermoplastic Polymer: Ensemble of entangled chains.
b) Thermoset Polymer: Cross-linked chains
Adapted from Singh (2015)

Figure 1.2 Molecular Arrangement: Thermoplastic vs Thermoset

Thermosets tend to have higher temperature resistance and do not suffer from creeping or warping at high temperatures, meaning that their mechanical properties are not severely temperature-dependent below the decomposition temperature. Due to their lower viscosity, thermosets are sought as they provide a better fibre impregnation before processing. Thermoplastics mechanical properties, on the other hand, tend to be tougher and a d less brittle than thermosets. However, their properties are more temperature-dependent, since they soften when heated.

1.2.1 Thermoplastics: Amorphous and Semi-crystalline Structure

Thermoplastics can be further categorized into amorphous and semi-crystalline polymers. Amorphous polymers have all of their chain molecules arranged in a random manner, while semi-crystalline polymers have part of their chain molecules arranged in an orderly structure

within an amorphous region, as shown in Figure 1.3 a [Yan & Shi (2011)]. This main difference has a significant impact on the polymer behaviour under heat.

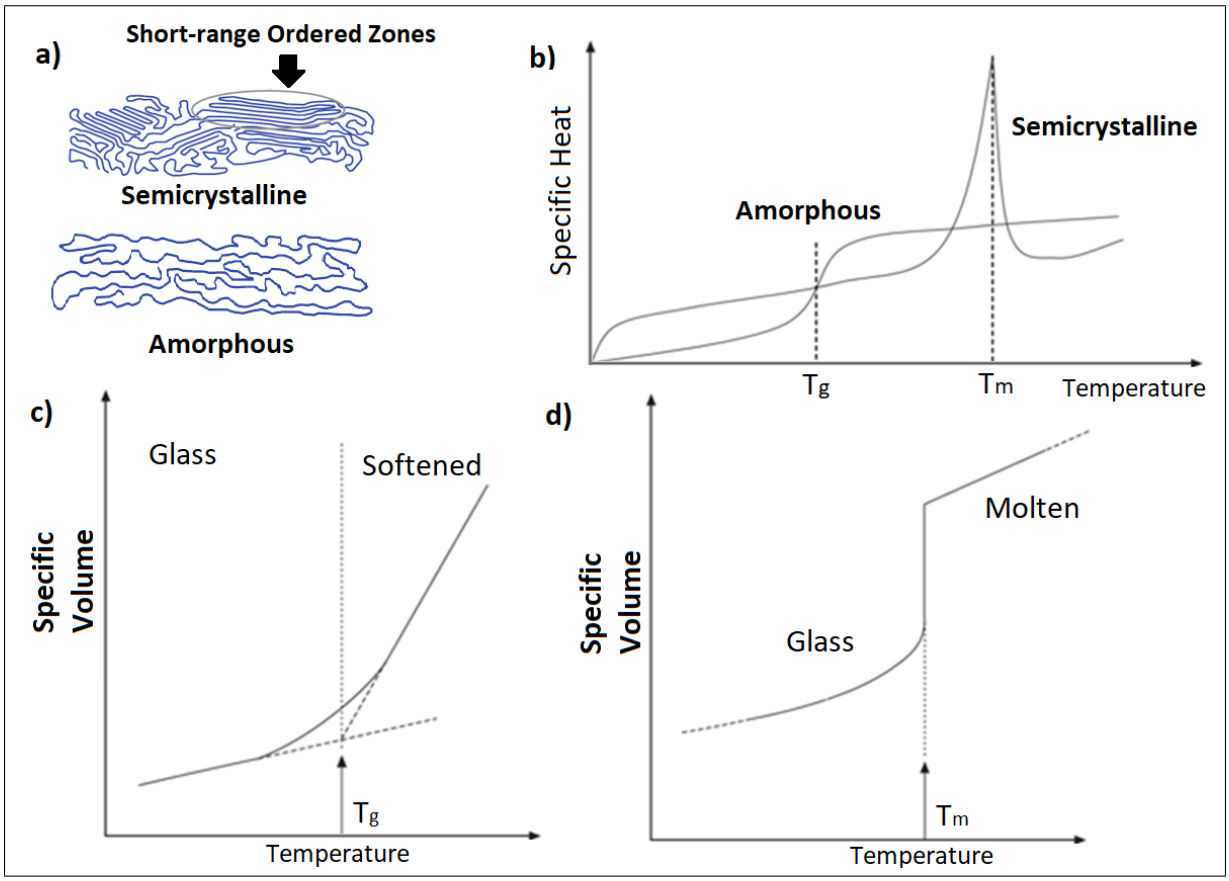

a) Semi-crystalline polymers show packed and organized polymer chains within amorphous regions, while amorphous materials show a disordered molecular arrangement. b) Specific heat of amorphous and semi-crystalline polymers. c) Amorphous behaviour: smooth specific volume change at the glass transition temperature. d) Semi-crystalline behaviour: sharp volume change at the melting temperature.
Adapted from Sastri (2010), Jones (2013) and Troughton (2009).

Figure 1.3 Amorphous and Semi-crystalline Thermoplastics Comparison.

Amorphous thermoplastics are characterized by the existence of a narrow temperature interval in which they change from a hard and brittle condition (sometimes called glassy) to a viscous fluid or rubbery state [Jones (2013)]. Within this temperature interval, it is defined a glass transition temperature T_g as shown in Figures 1.3.b and 1.3.c. Since movement of whole polymer chain

segments, material flow, is a necessary prerequisite of welding, amorphous thermoplastics need to be heated above T_g before welding takes place [Jones (2013)].

Semi-crystalline polymers have short-range ordered zones that can stack or align together to form ordered and compacted crystalline structures encompassed by amorphous regions [Sastri (2010)], as shown in Figure 1.3.a. It is convenient to highlight that the same thermoplastic can have different crystallinity degrees or levels - corresponding to the amount of short-range ordered zones - depending on the processing parameters. Due to these short-range ordered zones, semi-crystalline thermoplastics have a sharp melting temperature T_m, which is the temperature in which all the crystalline regions are molten.

When semi-crystalline polymers are heated, a gradual glass-transition of the amorphous phase is first observed. With further heating, the ordered compacted chains (crystalline phase) melt at the melting temperature T_m, as shown in Figure 1.3.b and 1.3.d. In order tp have resin flow, heating semi-crystalline thermoplastics above T_m is a prerequisite for welding.

Some other comparative characteristics between amorphous and semi-crystalline thermoplastics are found in table 1.1:

Table 1.1 Amorphous vs Semi-crystalline Characteristics

Property	**Amorphous**	**Semi-crystalline**
Optical	Typically transparent, clear	Typically translucent, opaque
Softening Point	Broad and gradual softening region	Sharp melting point
Shrinkage	Low	High anisotropic
Chemical Resistance	Poor	Good
Heat Resistance	Lower	Higher

1.3 Traditional Joining Methods vs Thermoplastic Welding

The design of large and/or complex structures would preferably avoid joints as they are potential sources of weakness and additional weight. Nevertheless, experiences available in the composite industry showed that the most cost-effective and viable method to design such structures often involves manufacturing multiple parts and assembling them together [Ageorges, Ye & Hou (2001)]. However, using traditional joining methods to assemble thermoplastic composites parts is difficult, labour intensive and costly.

Mechanical fastening methods exhibit problems arising from stress concentrations, thermal expansion coefficient mismatch and fabric damage induced by drilling, in addition to the negative impact of increased weight from the fasteners [Yousefpour, Hojjati & Immarigeon (2004)]. Adhesive bonding, which is mostly used for thermoset parts, is incompatible with thermoplastic resins due to the difficulty in bonding adhesive materials (often thermosets) to thermoplastic polymers.

To prevent these issues related to traditional techniques, welding, also known as fusion bonding, is considered as the most suitable process for joining thermoplastic composite parts. This process takes the advantage of uniform stress distribution, less sensitive to surface treatment, short cycle times and cost-effective process, as reported by the Defense and Space Group of the Boeing Company in which labour savings greater than 61% could be obtained by fusion bonding (welding) a composite wing structure as compared to a bolted one [Yousefpour *et al.* (2004)].

CHAPTER 2

CONSOLIDATION OF THERMOPLASTIC POLYMERS

Consolidation is a critical step in the manufacturing of thermoplastic welded parts, in which complex multi-physical phenomena takes place, such as resin flow, intimate contact development and molecular interdiffusion [Ageorges, Ye, Mai & Hou (1998)]. It is characterized by an isothermal condition with sharp fluctuations in the applied pressure for short periods of time [Roychowdhury & Advani (1991)].

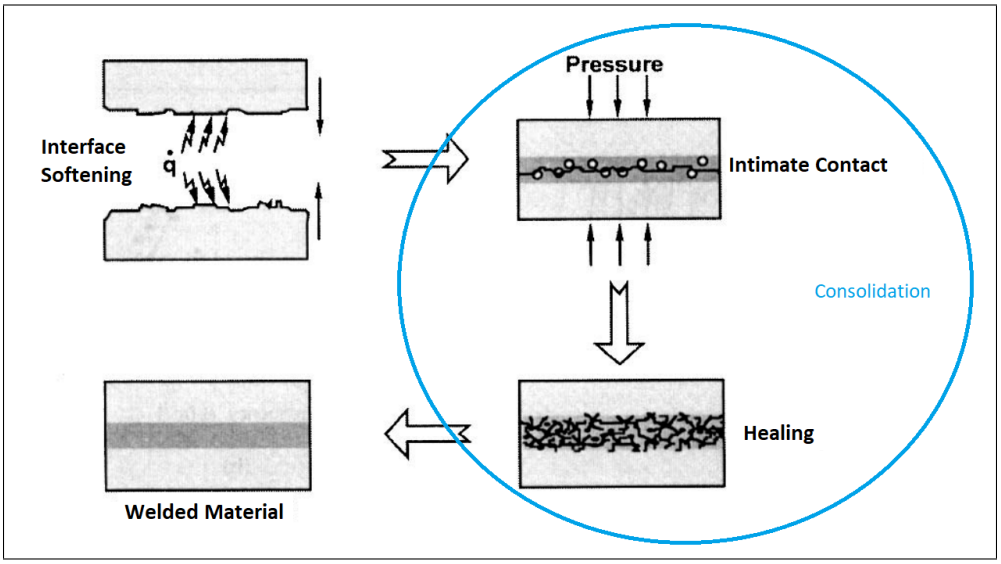

First, the adherents are heated in order to soften the thermoplastic material. Then, intimate contact is achieved by external pressure application. Simultaneously, healing occurs across the surfaces that are into intimate contact. Finally, a bulk material is obtained after cooling down.
Adapted from: Yang & Pitchumani (2002a)

Figure 2.1 Thermoplastic welding process

Due to the high viscosity of thermoplastic polymers, even at elevated temperatures, application of external pressure is essential to smooth out the adherent's rough surfaces, squeezing out volatiles and consequently developing an intimate contact between them. Simultaneously, macromolecules diffuse through interfaces that are into intimate contact, a phenomenon known

by healing or autohesion (Figure 2.1). A bulk material is thus obtained from two or more adherents.

Some modelling strategies used to describe the consolidation step, including both intimate contact and healing. A traditional viscous solid approach is presented. First, a Thermal Framework is described (section 2.1) as is vital in order to compute thermal field and history. Secondly, an Intimate Contact Framework is depicted (section 2.2) and highlighting the main modes that are used in order to study the roughness deformation in function of temperature and external applied pressure. Finally, a Healing Framework is considered (section 2.3) in order to investigate the weldline strength build up, which is mainly driven by the macromolecules diffusion through the weld interface.

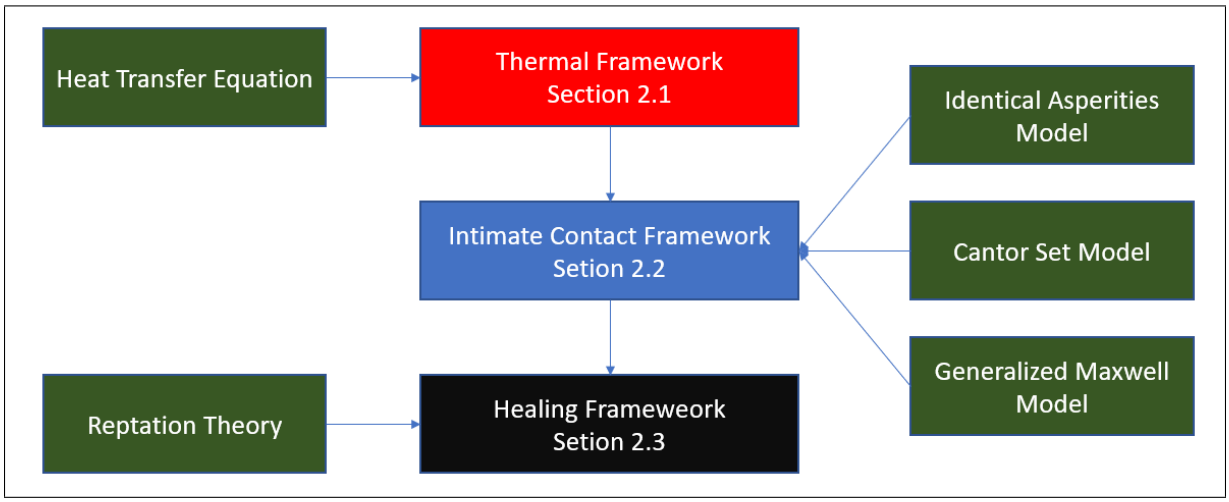

Models that are suitable to analyze the consolidation step from a viscous solid approach.

Figure 2.2 Consolidation Modelling: Frameworks and Models

Consolidation of thermoplastic welding involves more than one phenomenon in order to develop a weldline strength. At this section, the thermoplastic material is considered as a viscoelastic solid. First, a thermal framework is presented in order to evaluate the temperature field and history (section 3.1.1). Secondly, an intimate contact framework is depicted in order to evaluate the contact between rough surfaces.

2.1 Thermal Framework

Since the consolidation phase is only possible after heating the adherents above T_g or T_m (amorphous material for the first and semi-crystalline for the second), it is necessary to start the analysis from a thermal framework. The equation that represents the relation between heating and temperature (T) is the well-known heat transfer equation:

$$\rho(T) \cdot C_p(T) \frac{\partial T}{\partial t} = \nabla \cdot k(T) \nabla T + Q(t, T) \tag{2.1}$$

Thermal conductivity ($k(T)$) is the thermal property that determines ability of a material to conduct heat. Low thermal conductivity values render to insulator materials which hinder transfer heat and minimize heat losses. On the other hand, high thermal conductivity values render to conductive materials, which facilitate transferring heat from one site to another.

The specific heat ($C_p(T)$ - heat capacity per unit mass) is a thermodynamic quantity that determines the amount of heat necessary to raise by one degree the temperature of a unit mass of a material and is, therefore, associated with the energy absorption in heating processes. When semicrystlaline thermoplastics melt, C_p increases substantially (see Figure 1.3 d in chapter 1) since high energy absorbed by the semi-crystalline material is used up as latent heat and does not contribute towards a temperature variation [dos Santos, de Sousa & Gregorio (2013)].

The input heat density $Q(t, T)$ accounts for heat generated by the source $Q_s(t, T)$, heat generated during thermoplastic crystallization $Q_c(t, T)$ (in case of semi-crystalline) and latent heat that is

absorbed during matrix softening $Q_l(t,T)$ [Lionetto, Pappada, Buccoliero & Maffezzoli (2017)]. Thus, $Q(t,T)$ can be written as:

$$Q(t,T) = Q_s(t,T) + Q_c(t,T) - Q_l(t,T) \tag{2.2}$$

2.2 Intimate Contact Framework

When two laminates are brought into contact, voids will remain between the two surfaces because of their initial roughness. Due to the high viscosity of thermoplastic polymers, even at elevated temperatures, application of external pressure is essential to deform the material, spreading the roughness, squeezing out volatiles and developing an intimate contact between the adherents, as shown in Figure 2.3.

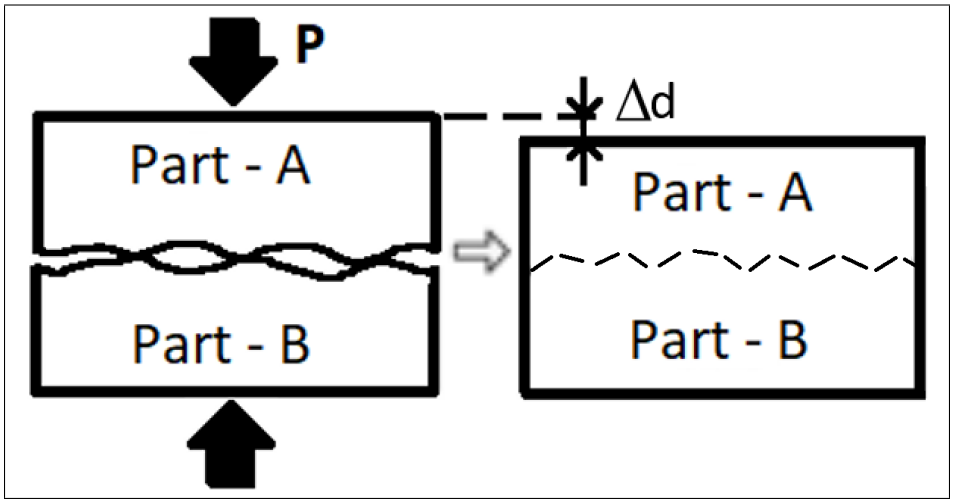

Two independent rough adherents are brought into contact. During the consolidation step, external pressure is applied, spreading the asperities and bringing them into intimate contact.
Adapted from Shi (2014)

Figure 2.3 Intimate contact

A thermoplastic material in its rubber state is assumed to behave as a viscoelastic solid. Viscoelasticity is the property of materials that exhibit both viscous and elastic characteristics

when undergoing deformation. A viscous material exhibits time-dependent stress-strain relation and when the load/displacement is removed, it remains in the deformed configuration. On the other hand, an elastic material has linear and instantaneous stress-strain relation and instantaneously return to its original configuration once the load/displacement is removed. Viscoelastic materials have elements of both of these properties and, as such, exhibit time-dependent strain showing a gradual time-dependent recover to their original configuration. [Papanicolaou & Zaoutsos (2011)]

Viscoelasticity is the property of materials that exhibit both viscous and elastic behaviour when undergoing deformation, resisting to shear flow and deforming when stress is applied, exhibiting a time-dependent stress and strain as shown in Figure 2.4.]

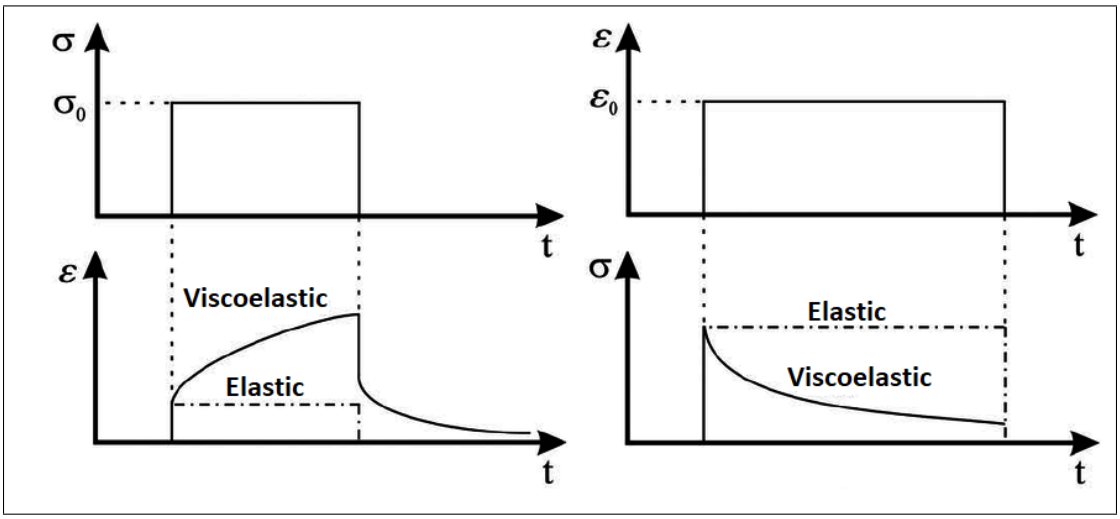

The creep test, on the left hand side figure, consists of measuring the time dependent strain ε resulting from the application of a steady uniaxial stress σ_0. The relaxation test consists of monitoring the time-dependent stress σ resulting from a steady strain ε_0 as seen the right hand side figure.

Figure 2.4 Viscoelasticity: creep and relaxation behaviours

Microscale - the scale of fibre, matrix and fibre/matrix interface - thermal analysis of the welding process has been reported [Mishra (2019)]. However, to the best of the author's knowledge, there is no available literature on the consolidation step microscale analysis of a thermoplastic

welding process, figuring the intimate contact development and subsequent healing. Therefore, the following models aim to describe the development of the intimate contact between two rough adherents considering homogenized materials.

2.2.1 Identical Asperities Model

Lee & Springer (1987) brought one simple analytical solution to describe the spreading of a rough surface approximating it by a series of periodic identical rectangular asperities, as it is shown in Figure 2.5.

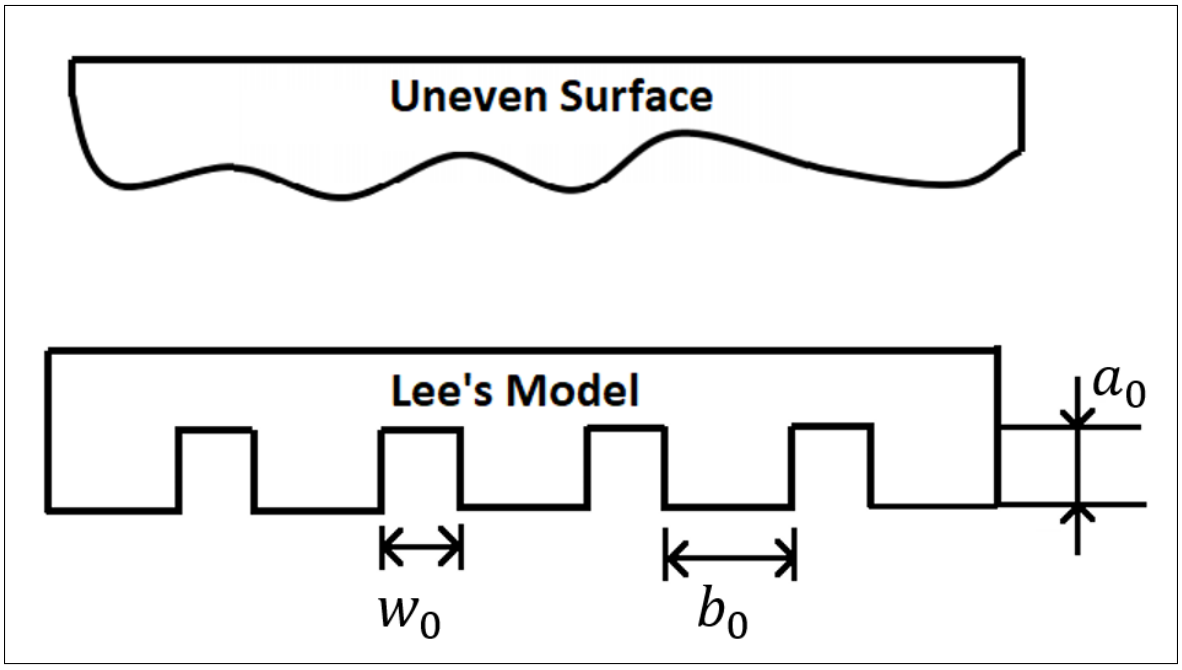

(a) Real-life roughness is approximated identical periodic rectangles.
Adapted from Xiong *et al.* (2019)

Figure 2.5 Lee and Springer‘s Model

By applying an external compressive pressure, the identical rectangular elements deform and smooth the rough surface along the interface bringing them into intimate contact. Mantell & Springer (1992) extended this model to account for time-varying properties and process

conditions (Temperature and Pressure). Based on their idealizations, the degree of intimate contact D_{ic} is expressed geometrically as:

$$D_{ic}(t) = \frac{b(t)}{w_0 b_0} \tag{2.3}$$

where w_o and b_0 are geometrical factors and are shown in Figure 2.5 and $b(t)$ is the width after pressure has been applied for a time t .

By assuming that the volume of each element remains constant, i.e $w + b = \text{cte}$, and applying the mass conservation law to a control volume of each element, Mantell & Springer (1992) obtained the following expression for the degree of intimate contact.

$$D_{ic} = D_{ic_0}\left[1 + C_1 \int_0^{t_p} \frac{P_{app}}{\mu_{mf(T)}} \mathrm{d}t\right]^{\frac{1}{5}} \tag{2.4a}$$

$$D_{ic_0} = \frac{1}{1 + \frac{w_0}{b_0}} \tag{2.4b}$$

$$C_1 = 5\left(1 + \frac{w_0}{b_0}\right)\left(\frac{a_0}{b_0}\right)^2 \tag{2.4c}$$

where D_{ic_0} represents the amount of area that is initially into intimate contact before any pressure is applied, and C_1 is a function of the size of the rectangular elements, μ_{mf} is the material viscosity, P_{app} is the applied pressure, t_p is the duration of the pressure cycle, and a_o is the idealized asperity height, as shown in Figure 2.5.

2.2.2 Cantor set Model

Since the representation of a rough surface as identical rectangles is a very simplified approach, Yang & Pitchumani (2001) proposed a more sophisticated analytical model known by Cantor

set Model, in which the multiple generations of rectangular asperities with decreasing height are considered as shown in Figure 2.6. In this model, the smallest asperities of the highest generation are squeezed without any deformation of the larger rectangles. Once the gaps of the highest generation are filled, the previous generation of asperities begins to deform. The full contact is reached as soon as the gaps of the first generation are filled.

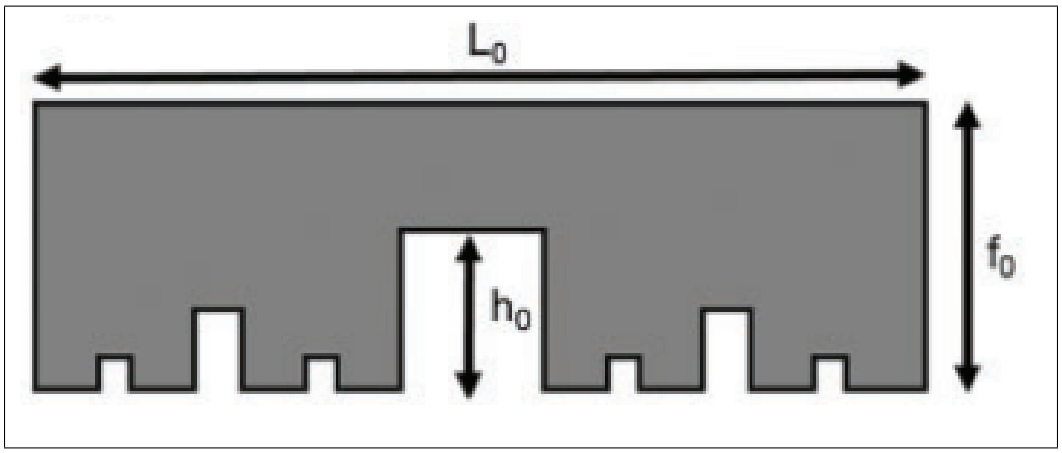

The first generation of asperities with height h_0 is shown. Subsequent generations have their height lower than the previous generation. Adapted from Yang & Pitchumani (2001)

Figure 2.6 Cantor set model

The evolution of intimate contact for the n_{th} generation of asperities is described by

$$D_{ic}^{n} = \frac{1}{f^{n}}\left[\frac{5}{4}\left(\frac{h_0}{L_0}\right)^{2}\frac{f^{\frac{2nD}{2-D}+n+4}}{(f+1)^{2}}\int_{t_{n+1}}^{t}\frac{P_{app}}{\mu_{mf(T)}}\mathrm{d}t+1\right]^{\frac{1}{5}} \tag{2.5}$$

in which the surface parameters for the Cantor set model are the fractal dimension of the surface D, the scaling ratio f, the height of the first generation asperity h_0 and the total horizontal length of the Cantor set block L_0 and can be directly obtained from the surface profile measurements.

2.2.3 Generalized Maxwell Model

Viscoelastic solid models based on discrete mechanical analogies of springs (elastic response) and dashpots (viscous response) were proposed by the literature since the 19th century. The two most accepted models are represented by Maxwell and Kevin-Voigt elements, which are shown in Figure 2.7.

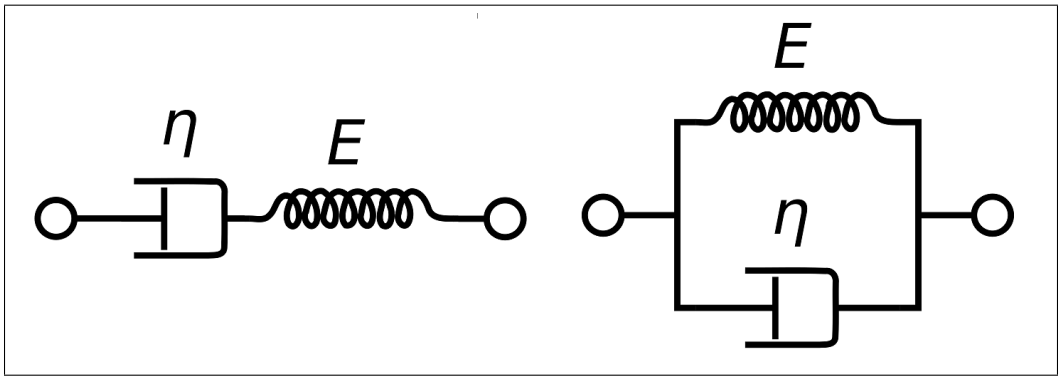

The left hand side shows the Maxwell element, composed by one dashpot and one spring in series. The right hand side shows the Kevin-Voigt element, composed by one dashpot and one spring in parallel.

Figure 2.7 Viscoelasticity Models

Linear viscoelastic behaviour can be accurately described using The Generalized Maxwell Element, which has proved to be a useful rheological structure to formulate time-dependent and frequency-dependent characteristics [Kaliske (2000)], as it can be calibrated to describe both linear relaxation and linear creep behaviour. Within this model, the material deformation is calculated in function of the internal viscoelastic stress, which is a response to the externally applied pressure. Once the deformation field is known, it is possible to track the evolution of the surface roughness and therefore calculate the degree of intimate contact D_{ic}.

A schematic representation of the Generalized Maxwell-element is shown in Figure 2.8. The isolated spring represents the final or equilibrium stiffness/stress, while the n_{th_s} individual Maxwell-element represents contributions of viscous stiffness/stress. All the branches are

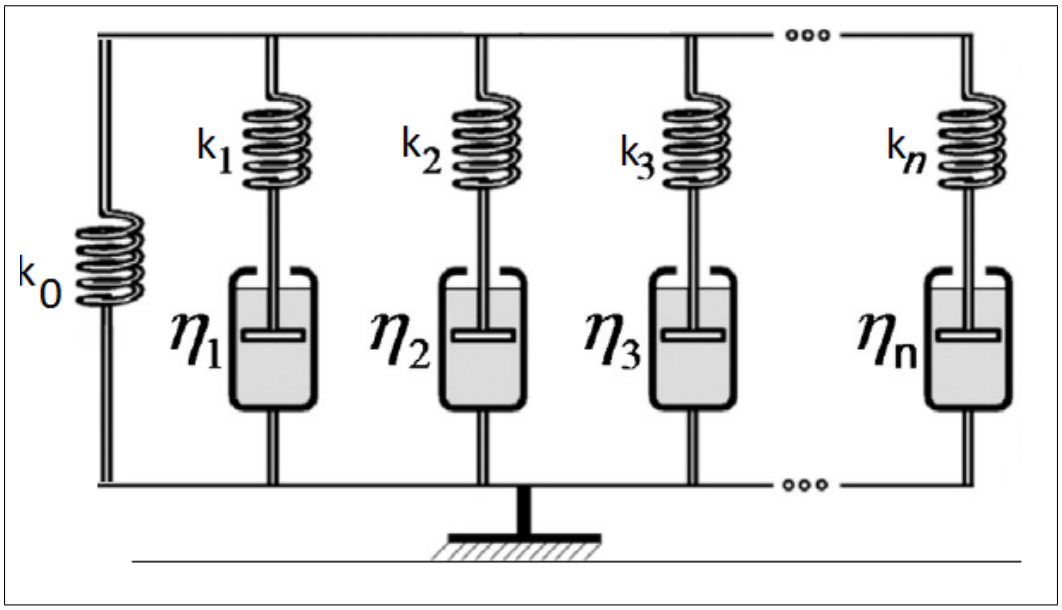

Isolate spring, representing the final or equilibrium stiffness/stress, in parallel with multiple Maxwell-elements representing the viscous stiffness/stress. All the branches have the same strain/displacement.

Figure 2.8 Generalized Maxwell Element

connected in parallel, meaning that they have the same strain $\varepsilon(t)$ at all times t. Thus, the overall stress of the system is the sum of the stresses in each branch, formed additively from purely elastic stress S_0 and viscoelastic stresses h_j.

$$\{S\} = \{S_0\} + \sum_{j=1}^{N} \{h_j\} \tag{2.6}$$

The parallel association of n-Maxwell elements leads to a relaxation function, which is essentially a Prony series with coefficients k_j and exponential decays proportional to the relaxation time $\tau_j = \frac{\eta_j}{k_j}$ of the j_{th} Maxwell-element as expressed by:

$$[\Gamma_t] = [k_0] + \sum_{j=1}^{J} [k_j] \, exp\left(-\frac{t}{\tau_j}\right) \tag{2.7}$$

where k_j and η_j are the spring and dashpots constants respectively. Here, k_0 is the final (or equilibrium) modulus and $k_0 + \sum_{j=1}^{J} k_j$ is the instantaneous modulus.

In the case of the consolidation step, an external compressive pressure is applied and the material deforms according to the stress-strain relation. Within this deformation, the rough surfaces are smoothed out, creating zones that are into intimate contact.

It is important to mention that no temperature dependency is considered here, since the formulation is based on isothermal condition. For numerical implementations based on forwarding steps, a numerical approximation is done in order to consider the anisothermal characteristic of the welding process. So, the material properties need to be described as a function of temperature and a isothermal condition is considered within each step. Then, the anisothermal condition is obtained by summing each sufficiently small isothermal steps.

2.2.4 Intimate Contact Framework: Conclusions and Limitations

As discussed, the first requirement for welding is the establishment of an intimate contact between the rough adherents, which is achieved by an external pressure and heat. In order to evaluate the evolution of this intimate contact, three models were discussed, firstly depicting two of the most found in the literature analytical models: Identical Asperities and Cantor Set Model. Comparing their formulation, it is concluded that the real-life surface is described in a similar way by an idealized geometry.

Finally, the Generalized Maxwell Model was introduced. In this model, the degree of intimate contact is evaluated in function of the material's deformation as a response to internal viscoelastic stress. Also, within this model, the anisothermal consolidation phenomenon can be solved considering isothermal steps if these steps are sufficiently small to sustain this hypothesis.

All models have the common limitation of being evaluated as homogenized material. For the best-knowledge of the author, no micromechanical analysis - scale in which fibre, matrix and fibre/matrix interface - on the consolidation of thermoplastic welding is available yet, leaving

an open gap to be explored. Moreover, none of the models consider a liquid-solid phase transformation, but instead a viscous (for the first two models) or viscoelastic solid (the last model).

Model	Input	Output	Comment and Limitation
Identical Asperities	a_0, b_0, P_{app}, μ_{mf}	D_{ic}	Real-life roughness is approximated by identical periodic rectangles.
Cantor Set	D, f, L_0, h_0, P_{app},μ_{mf}	D_{ic}	Real-life roughness is approximated by multi-generation rectangles.
Generalized Maxwell	$[k_0]$, $\left[k_j\right]$, τ_j	$\{u\}$	The anisothermal process is approximated by the sum of isothermal steps.

Table 2.1 Intimate Contact Framework

2.3 Autohesion Modelling

When two thermoplastic materials are into intimate contact, a chain interdiffusion across the interface is noticed, a process referred as healing or autohesion. Thus, the processes of intimate contact and healing are coupled in that healing can occur only across areas of the interface that are in intimate contact. While intimate contact development is a function of the applied pressure, temperature and time, healing is governed by the temperature history and time alone [Yang & Pitchumani (2003)].

De Gennes (1971) studied the chain motion in the bulk polymeric material, presenting the fundamentals of the reptation theory. The reptation model is suitable to describe the motion of a chain that is entangled with many other chains. This chain entanglement constrains single chains inside a tube-like region, in which are allowed to move back and forward along the curvilinear length of the tube [Kim & Wool (1983)]. In order to see how a single chain disengages itself from the initial tube, chain conformations at different times are shown in Figure 2.9.

At the beginning of the process, $t_0 = 0$, the chain, represented by the thin solid line in Figure 2.9, is totally encompassed by a tube, which represents the chain constraints imposed by the entanglement of neighboring chains. At a certain time $t = t_1$ the chain ends escape from the original tube, forming the "minor chains". The length, l, of the minor chain increases with time and reaches L at the reptation time t_r (when the entire polymer chain escapes from the tube).

Wool & OConnor (1981) extended the work of De Gennes (1971) expanding the molecular motion within the bulk to the motion of the molecular chains across a weld interface. Initially, two adherents are assumed to be in perfect contact at the interface, as shown in Figure 2.10 (note that only the molecules on one side of the interface are illustrated for clarity). At $t = t_0$, the chains do not have minor chains and therefore, are denoted by dots. As time proceeds, the lengths of the minor chains grow, and some of the chains move across the interface with an interpenetration distance χ, which contributes to build up a weldline strength.

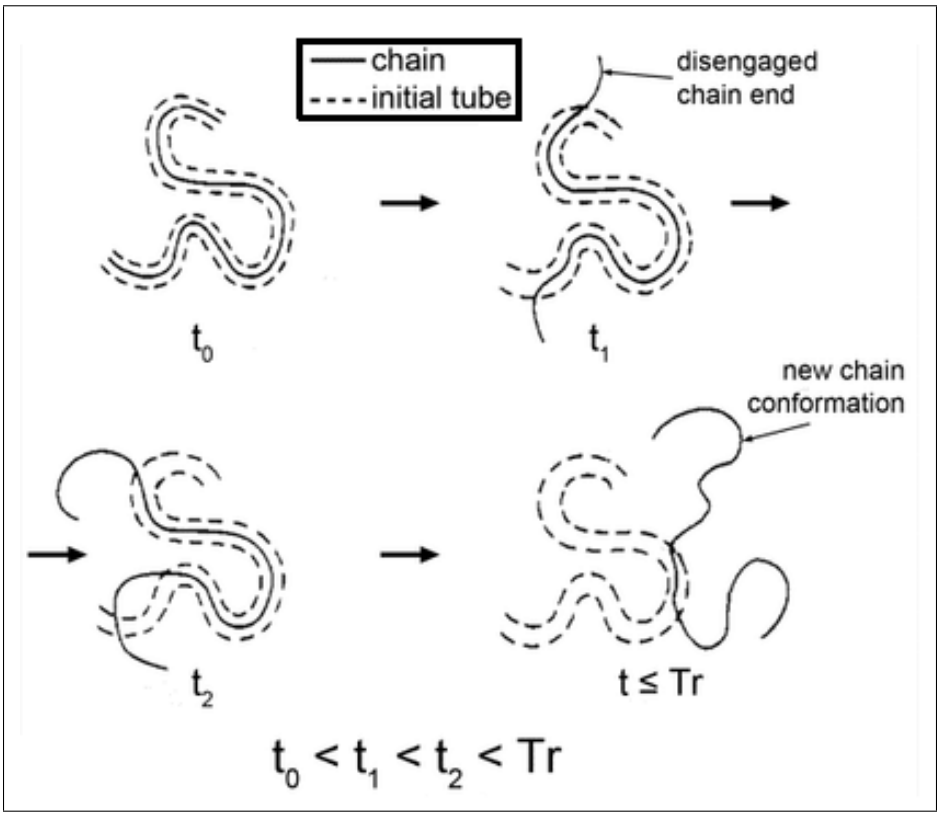

At the beginning of the process, t_0, the chain is totally encompassed by the tube. At a certain time t_1 the chain ends escape from the tube. This disengagement continues as time progresses (t_2), until the reptation time t_r is reached, when the entire polymer chain scapes from the tube, characterizing full healing.
Source: Yang & Pitchumani (2003)

Figure 2.9 Reptation Theory

At the reptation time, the interpenetration and entanglement of all the polymer chains are fully developed and the molecular configuration at the interface is identical to that of the virginal bulk material [Yang & Pitchumani (2002b)]. Keeping the rubbery material for times longer than the reptation time is unnecessary as it does not result in additional strength enhancement [Ezekoye *et al.* (1998)].

The interlaminar bond strength, σ, is proportional to the interpenetration depth χ, which is related to the minor chain length $\chi \sim \sqrt{l}$. The ultimate bond strength, σ_∞, is achieved when

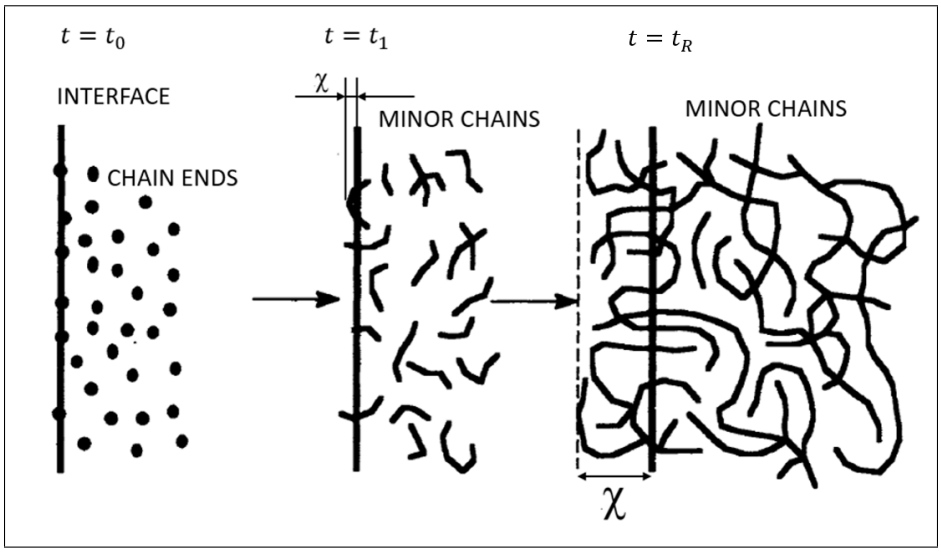

At the beginning of the process, $t = t_0$, the minor chains have zero length. As time proceeds, the lengths of the minor chains grow ($t = t_1$) and some of them move across the interface ($t = t_r$). Adapted from: Ezekoye *et al.* (1998)

Figure 2.10 Polymer chain diffusion across the weld interface

the interpenetration depth and the minor chain length reach their maximum values χ_∞ and L, respectively. Under isothermal conditions the time-relation of minor chain length grow l is expressed as:

$$\frac{l}{L} = \left(\frac{t}{t_r}\right)^{\frac{1}{2}} \tag{2.8}$$

Thus, the degree of healing may be defined as the ratio of the instantaneous interfacial bond strength to the ultimate bond strength as:

$$D_{au}(t) = \frac{\sigma(t)}{\sigma_\infty} = \frac{\chi(t)}{\chi_\infty} = \left(\frac{l}{L}\right)^{\frac{1}{2}} = \left(\frac{t}{t_r}\right)^{\frac{1}{4}} \tag{2.9}$$

Kim & Wool (1983) suggested that for high molecular weight thermoplastics (which is the case of most thermoplastics used in high-performance systems), the interpenetration depth and minor chain length do not have to reach their maximum values (χ_∞ and L respectively) to obtain maximum bond strength. Instead, it is achieved at the welding time t_w, which is lower than t_r [Yang & Pitchumani (2003)], resulting in the following relations:

$$t_w < t_r \tag{2.10a}$$

$$\chi_w < \chi_\infty \tag{2.10b}$$

$$L_w < L \tag{2.10c}$$

Thus, a general expression for the degree of healing using the parameters at the welding time follows. Note that Equation 2.11 is similar to Equation 2.9 if $t_w = t_r$, which is the case for low molecular weight thermoplastics.

$$D_{au}(t) = \frac{\sigma(t)}{\sigma_\infty} = \frac{\chi(t)}{\chi_w} = \left(\frac{l(t)}{L_w}\right)^{\frac{1}{2}} = \left(\frac{t}{t_w}\right)^{\frac{1}{4}} \tag{2.11}$$

Bastien & Gillespie Jr. (1991) extended the reptation theory to account the anisothermal condition of a fusion bonding process. In their model, the temporal domain of a nonisothermal healing process was divided into q time intervals and the process in each i_{th} interval was considered to be isothermal $T_i^\star$at the average of the temperatures between t_i and t_{i+1}. The incremental bond strengths accumulated within each Δt is derived from the isothermal reptation theory. Thus the degree of healing at any step i is determined by a summation of the incremental strength values [Yang & Pitchumani (2002b)].

$$D_{au}(t_i) = \frac{\sigma(t_i)}{\sigma_\infty} = \sum_{t=0}^{\frac{t}{\Delta t}} \frac{t_{i+1}^{\frac{1}{4}} - t_i^{\frac{1}{4}}}{t_w^{\star\,\frac{1}{4}}} \tag{2.12}$$

The foregoing nonisothermal extension of the healing model seems to be plausible and in fact has been widely accepted and used in modelling fabrication processes. However, it is observed that the above equation is truly valid if the process is isothermal within the step. Since this does not represent the thermal history during actual processing conditions Yang & Pitchumani (2002b) developed an integral formulation to incorporate the anisothermal healing, yielding:

$$D_{au}(T,t) = \left[\int_0^{t_f} \frac{1}{t_w(T)}\mathrm{d}t\right]^{\frac{1}{4}} \tag{2.13}$$

It is important to highlight that the whole theory was built for amorphous thermoplastics. As suggested by Lee & Springer (1987), the degree of crystallinity affects the accuracy of Eq. 2.13, as the crystalline ordered structures act as obstacles to the motion of the chains and healing. If healing is controlled by diffusion, then the bondline strength of an amorphous/amorphous interface should develop faster than that of a crystalline/crystalline since the central portion of the chains are firmly fixed within the crystals for the latter [Boiko, Guérin, Marikhin & Prud'homme (2001)]. Figure 2.11 shows how this phenomenon can impact the strength of Polyethylene Terephthalate (PET) polymers.

Nonetheless this model has been widely used to model auto-adhesion in forming processes of semi-crystalline matrix composites. Thus, it is possible that this value is well overestimated since crystallization is likely to affect healing. To account for this limitation, a full multi-physical model predicting the melting and crystallization phenomenon should be considered [Levy, Le Corre & Poitou (2014)].

Autohesion Framework: Conclusions and Limitations

When two thermoplastic polymer surfaces are joined by welding, strength is developed by the diffusion of polymer chains across the welding interface and when full healing occurs, the welded material has strength equal to that of the polymer bulk. This phenomenon can be explained by the reptation theory, in which the bondline strength is given in function of temperature, time

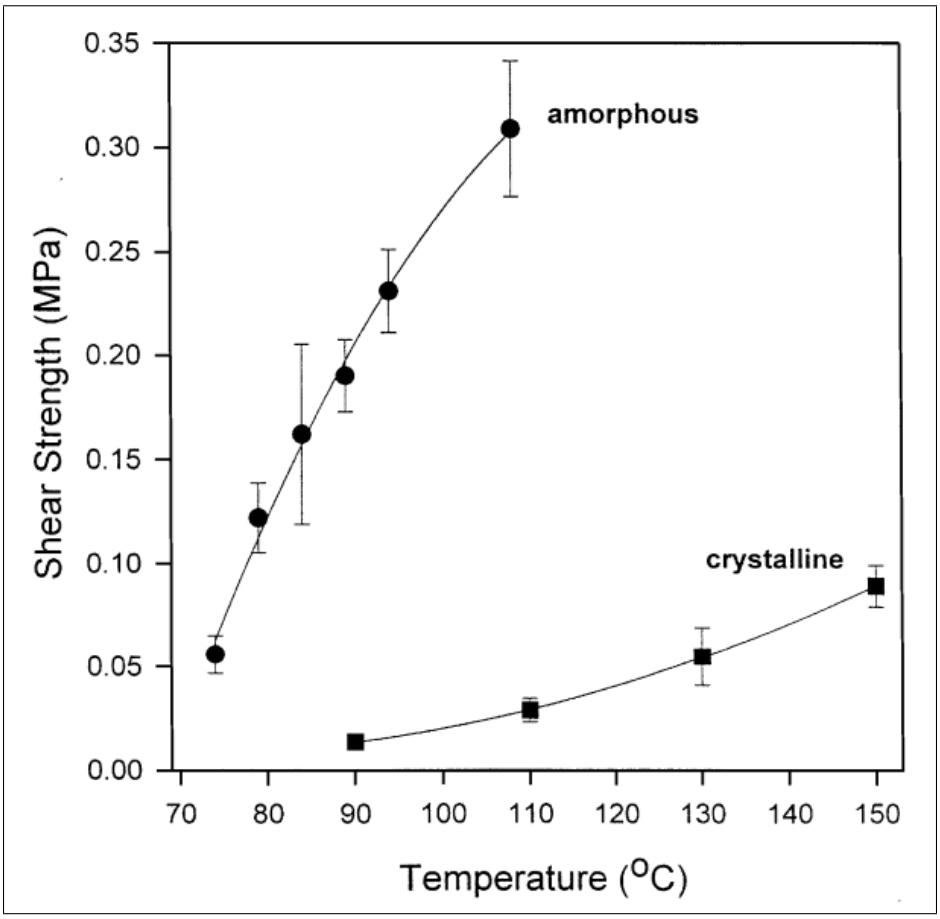

Amorphous/amorphous interface healing develops higher strength than crystalline/crystalline interface: Crystalline ordered structures act as obstacles to the chains motion, affecting the bondline strength. Source: Boiko *et al.* (2001)

Figure 2.11 Shear strength as function of healing temperature at amorphous/amorphous and crystalline/crystalline PET

and material properties, such as welding time and interpenetration depth. Despite a simple formulation, this model does not take into consideration crystallinity effects.

Model	Input	Output	Comment
Reptation Model	$t_w(T)$	$D_h(t)$	Homogeneous medium, no crystallinity effects

Table 2.2 Autohesion Framework

REFERENCES

Ageorges, C., Ye, L. & Hou, M. (2001). Advances in fusion bonding techniques for joining thermoplastic matrix composites: a review. *Composites Part A: Applied Science and Manufacturing*, 32(6), 839 - 857. doi: https://doi.org/10.1016/S1359-835X(00)00166-4.

Ageorges, C., Ye, L., Mai, Y.-W. & Hou, M. (1998). Characteristics of resistance welding of lap shear coupons.: Part II. Consolidation. *Composites Part A: Applied Science and Manufacturing*, 29(8), 911 - 919. doi: https://doi.org/10.1016/S1359-835X(98)00023-2.

Bastien, L. J. & Gillespie Jr., J. W. (1991). A non-isothermal healing model for strength and toughness of fusion bonded joints of amorphous thermoplastics. *Polymer Engineering & Science*, 31(24), 1720-1730. doi: 10.1002/pen.760312406.

Bîrca, A., Gherasim, O., Grumezescu, V. & Grumezescu, A. M. (2019). Introduction in thermoplastic and thermosetting polymers. *Materials for Biomedical Engineering: Thermoset and Thermoplastic Polymers*, 1–28. doi: 10.1016/B978-0-12-816874-5.00001-3.

Boiko, Y. M., Guérin, G., Marikhin, V. A. & Prud'homme, R. E. (2001). Healing of interfaces of amorphous and semi-crystalline poly(ethylene terephthalate) in the vicinity of the glass transition temperature. *Polymer*, 42(21), 8695 - 8702. doi: https://doi.org/10.1016/S0032-3861(01)00406-2.

Cervenka, A. (1999). Advantages and Disadvantages of Thermoset and Thermoplastic Matrices for Continuous Fibre Composites. *Mechanics of Composite Materials and Structures*, 289–298. doi: doi.org/10.1007/978-94-011-4489-6_16.

De Gennes, P. G. (1971). Reptation of a polymer chain in the presence of fixed obstacles. *The Journal of Chemical Physics*, 55(2), 572–579. doi: 10.1063/1.1675789.

dos Santos, W., de Sousa, J. & Gregorio, R. (2013). Thermal conductivity behaviour of polymers around glass transition and crystalline melting temperatures. *Materials Today: Proceedings*, 32(5), 987 - 994. doi: https://doi.org/10.1016/j.polymertesting.2013.05.007.

Ezekoye, O. A., Lowman, C. D., Fahey, M. T. & Hulme-Lowe, A. G. (1998). Polymer weld strength predictions using a thermal and polymer chain diffusion analysis. *Polymer Engineering and Science*, 38(6), 976–991. doi: 10.1002/pen.10266.

International Air Transport Association - IATA. (2019). Aircraft Technology Roadmap to 2050.

Jones, I. (2013). *Laser welding of plastics*. Woodhead Publishing Limited. doi: 10.1533/9780857098771.2.280.

Kaliske, M. (2000). A formulation of elasticity and viscoelasticity for fibre reinforced material at small and finite strains. *Computer Methods in Applied Mechanics and Engineering*, 185, 225-243. doi: 10.1016/S0045-7825(99)00261-3.

Kim, Y. H. & Wool, R. P. (1983). A Theory of Healing at a Polymer Polymer Interface. *Macromolecules*, 16(7), 1115–1120. doi: 10.1021/ma00241a013.

Lee, W. I. & Springer, G. S. (1987). A Model of the Manufacturing Process of Thermoplastic Matrix Composites. *Journal of Composite Materials*, 21(11), 1017-1055. doi: 10.1177/002199838702101103.

Levy, A., Le Corre, S. & Poitou, A. (2014). Ultrasonic welding of thermoplastic composites: A numerical analysis at the mesoscopic scale relating processing parameters, flow of

polymer and quality of adhesion. *International Journal of Material Forming*, 7, 39-51. doi: 10.1007/s12289-012-1107-6.

Lionetto, F., Pappada, S., Buccoliero, G. & Maffezzoli, A. (2017). Finite element modeling of continuous induction welding of thermoplastic matrix composites. *Materials & Design*, 120, 212-221. doi: 10.1016/j.matdes.2017.02.024.

Llorca, J., González, C., Molina-Aldareguia, J. & Lopes, C. (2012). Multiscale Modeling of Composites: Toward Virtual Testing ... and Beyond. *JOM*, 65, 1-11. doi: 10.1007/s11837-012-0509-8.

Mantell, S. C. & Springer, G. S. (1992). Manufacturing Process Models for Thermoplastic Composites. *Journal of Composite Materials*, 26(16), 2348-2377. doi: 10.1177/002199839202601602.

Mishra, K. (2019). *From the determination of thermal properties of fibers to multiscale modeling of heat transfer in composite*. (Ph.D. thesis).

Papanicolaou, G. & Zaoutsos, S. (2011). 1 - Viscoelastic constitutive modeling of creep and stress relaxation in polymers and polymer matrix composites. In Guedes, R. M. (Ed.), *Creep and Fatigue in Polymer Matrix Composites* (pp. 3 - 47). Woodhead Publishing. doi: https://doi.org/10.1533/9780857090430.1.3.

Roychowdhury, S. & Advani, S. (1991). Characterization of consolidation in thermoplastic matrix composites. doi: 10.2514/6.1991-933.

Sastri, V. R. (2010). Materials Used in Medical Devices. *Plastics in Medical Devices*, 21–32. doi: 10.1016/b978-0-8155-2027-6.10003-0.

Shi, H. (2014). *Resistance welding of thermoplastic composites – process and performance*. (Ph.D. thesis).

Singh, A. (2015). Drilling of Glass Fiber Reinforced Polymer (GFRP) Composites: Parametric Appraisal and Multi Response Optimization.

Troughton, M. J. (2009). Chapter 2 - Ultrasonic Welding. In Troughton, M. J. (Ed.), *Handbook of Plastics Joining (Second Edition)* (ed. Second Edition, pp. 15 - 35). Boston: William Andrew Publishing. doi: https://doi.org/10.1016/B978-0-8155-1581-4.50004-4.

Wool, R. & OConnor, K. (1981). Crack Healing In Polymers. *Journal of Applied Physics*, 52, 5953 - 5963. doi: 10.1063/1.328526.

Xiong, H., Hamila, N. & Boisse, P. (2019). Consolidation Modeling during Thermoforming of Thermoplastic Composite Prepregs. *Materials*, 12, 2853. doi: 10.3390/ma12182853.

Yan, C. & Shi, Y. (2011). Investigation into the Differences in the Selective Laser Sintering between Amorphous and Semi-crystalline Polymers. *International Polymer Processing Journal of the Polymer Processing Society*, 26. doi: 10.3139/217.2452.

Yang, F. & Pitchumani, R. (2001). Fractal Description of Interlaminar Contact Development during Thermoplastic Composites Processing. *Journal of Reinforced Plastics and Composites - J REINF PLAST COMPOSITE*, 20, 536-546. doi: 10.1106/DAEQ-L4HD-N45W-4MJR.

Yang, F. & Pitchumani, R. (2002a). Interlaminar contact development during thermoplastic fusion bonding. *Polymer Engineering & Science*, 42, 424 - 438. doi: 10.1002/pen.10960.

Yang, F. & Pitchumani, R. (2002b). Healing of Thermoplastic Polymers at an Interface under Nonisothermal Conditions. *Macromolecules*, 35. doi: 10.1021/ma010858o.

Yang, F. & Pitchumani, R. (2003). Nonisothermal Healing and Interlaminar Bond Strength Evolution During Thermoplastic Matrix Composites Processing. *Polymer Composites*, 24, 263 - 278. doi: 10.1002/pc.10027.

Yousefpour, A., Hojjati, M. & Immarigeon, J.-P. (2004). Fusion Bonding/Welding of Thermoplastic Composites. *Journal of Thermoplastic Composite Materials - J THERMOPLAST COMPOS MATER*, 17, 303-341. doi: 10.1177/0892705704045187.